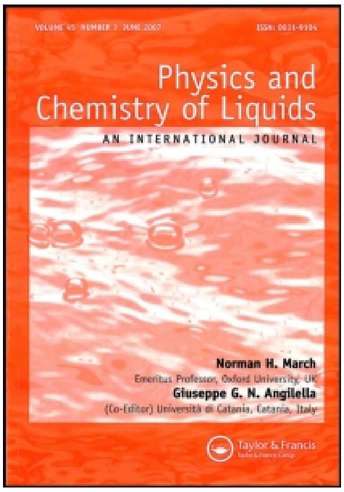

Physics and Chemistry of Liquids
Publication details, including instructions for authors and subscription information:
http://www.informaworld.com/smpp/title~content=t713646857

Chemical Short Range Order in Molten MnCu and MnSn Alloys of the Null-Matrix Composition

Ji-Chen Li[a]; N. Cowlam[a]; F. He Fenglai[ab]
[a] Department of Physics, University of Sheffield, Sheffield, UK [b] Department of Basic Science, Shanghai Building Material Institute, Jiangwan, Shanghai, Peoples Republic of China

To cite this Article Li, Ji-Chen , Cowlam, N. and Fenglai, F. He(1988) 'Chemical Short Range Order in Molten MnCu and MnSn Alloys of the Null-Matrix Composition', Physics and Chemistry of Liquids, 18: 1, 31 — 41
To link to this Article: DOI: 10.1080/00319108808078575
URL: http://dx.doi.org/10.1080/00319108808078575

Phys. Chem. Liq., 1988, Vol. 18, pp. 31-41
Photocopying permitted by license only
Reprints available directly from the publisher

Printed in the United Kingdom

Chemical Short Range Order in Molten MnCu and MnSn Alloys of the Null-Matrix Composition

JI-CHEN LI, N. COWLAM and F. HE FENGLAI*

Department of Physics, University of Sheffield, Sheffield S3 7RH, UK

(Received 17 September 1987)

Neutron diffraction experiments have been made on molten alloys $Mn_{67.4}Cu_{32.6}$ and $Mn_{62.6}Sn_{37.4}$ which have the "null-matrix" composition. The scattered intensity distributions for these alloys have been corrected for paramagnetic neutron scattering and they then relate to composition fluctuations alone. They have been analysed to yield the Radial Concentration Function (RCF). The RCFs for both alloys give a clear indication of true short range order—a preference for unlike first neighbours. The curves are discussed in terms of expected first neighbour distances and the atomic correlations in the stable crystalline phases. Comparison is also made between the values of the chemical short range order parameter α_1 estimated from the RCFs and the measured values of the enthalpy of mixing ΔH.

KEY WORDS: Null-matrix composition, molten alloys, radial concentration function.

1 INTRODUCTION

There has been considerable interest recently, in metallic alloy glasses, produced by fast quenching liquid metal alloys. Several excellent determinations of the structures of metallic alloy glasses have been made (see Ref. 1) against which structural models and simulations may be compared. Experiments on the equivalent molten alloys are important in providing evidence for precursors of those mechanisms which are thought to influence the glassy structures. Chemical short range order (CSRO) between the alloy constituents has been demonstrated to correlate with the stability of Cu-Ti metallic glasses.[2] Measurements on

---

* Permanent address: Department of Basic Science, Shanghai Building Material Institute, 100 Wudong Road, Jiangwan, Shanghai, Peoples Republic of China.

liquid CuTi alloys have also shown that CSRO exists in the liquid state, that it follows the same trend with composition which occurs in the glasses and that it is enhanced on vitrification.[3]

It is not surprising that CSRO should be present in metallic glass structures since strong heterogeneous interactions between the alloy constituents in the melt, determine the eutectics in the phase diagrams which can frequently be associated with good glass-forming ability.[4] However for the maximum sensitivity to CSRO, neutron diffraction measurements on alloys in which one of the constituents exhibits the so-called "negative scattering" are needed. Unfortunately the two transition metals, titanium and manganese which exhibit this in their elemental form (without isotopic enrichment) are quite reactive. Their alloys are difficult to contain in the liquid state, particularly when the choice of container is influenced by extra considerations of neutron scattering and transmission.[3] This makes it difficult to extend these diffraction experiments. The authors have therefore begun exploratory neutron diffraction work on manganese and titanium-based alloys which are experimentally accessible in having reasonably low melting points. The present report concerns neutron measurements on $Mn_{67.4}Cu_{32.6}$ and $Mn_{62.6}Sn_{37.4}$ molten alloys of the "null-matrix" composition.

2 EXPERIMENTAL METHOD AND DATA ANALYSIS

2.1 Null-Matrix Alloys

The most convenient formalism for discussing CSRO in disordered systems is that due to Bhatia and Thornton.[5] The total structure factor $S(Q)$ is defined from the corrected intensity of scattering per atom

$$I(Q) = \langle b^2 \rangle S(Q) \tag{1}$$

and can be expressed in terms of three partial structure factors (PSFs)

$$\langle b^2 \rangle S(Q) = \langle b \rangle^2 S_{NN}(Q) + 2\langle b \rangle \Delta b\, S_{NC}(Q) + (\Delta b)^2 S_{CC}(Q) \tag{2}$$

Here b is the nuclear scattering amplitude, $\langle b \rangle = xb_A + (1-x)b_B$, $\langle b^2 \rangle = xb_A^2 + (1-x)b_B^2$ and $\Delta b = b_A - b_B$ for an A_xB_{1-x} binary alloy. $S_{NN}(Q)$ is the number-number PSF, relating to density variations, its Fourier transform gives the Radial Distribution Function, RDF $4\pi r^2 \rho_{NN}(r)$ from which the co-ordination number is obtained. $S_{CC}(Q)$ is the concentration-concentration PSF relating to compositional fluctuations and has a limiting value $x(1-x)$. The Fourier transform of $S_{CC}(Q)/x(1-x)$ gives the radial concentration function $4\pi r^2 \rho_{CC}(r)$

(RCF) which oscillates about zero. Positive peaks in the RCF correspond to like-atom correlations and negative peaks to unlike correlations. The CSRO parameter,[6] α_1 for the first shell of neighbours can be obtained from the area of the first peak $(\alpha_1 n_1)$ if the co-ordination number n_1 is known.[7] $S_{NC}(Q)$ is a "size-effect" cross term for density variations stimulated by chemical fluctuations (and vice versa).

It can be seen that when one constituent of a binary alloy has a negative value of b then

$$\langle b \rangle = x_{nm} b_A + (1 - x_{nm}) b_B = 0 \tag{3}$$

at the so-called "null-matrix" composition x_{nm}, so that

$$\langle b^2 \rangle S(Q) = (\Delta b)^2 S_{CC}(Q) \tag{4}$$

In this case the neutron scattering relates to composition fluctuations alone. Given the values[8] $b_{\mathrm{Mn}} = -0.373 \times 10^{-12}$ cm, $b_{\mathrm{Cu}} = 0.772 \times 10^{-12}$ cm, $b_{\mathrm{Sn}} = 0.623 \times 10^{-12}$ cm this occurs at compositions $\mathrm{Mn}_{67.4}\mathrm{Cu}_{32.6}$ and $\mathrm{Mn}_{62.6}\mathrm{Sn}_{37.4}$ respectively.

2.2 Neutron Experiments and Their Analysis

Parent alloy ingots having composition $\mathrm{Mn}_{67.4}\mathrm{Cu}_{32.6}$ and $\mathrm{Mn}_{62.6}\mathrm{Sn}_{37.4}$ were prepared by argon-arc melting of spectroscopically pure constituents with negligible weight loss. The ingots were machined to fit into thin-walled quartz containers (ϕ = 8 mm) which prior tests had shown were appropriate to hold the specimens. The neutron experiments were made using the Curran diffractometer at DIDO reactor (25 MW) at A.E.R.E. Harwell. The samples were measured in a conventional furnace with a tantalum heater element. The $\mathrm{Mn}_{67.4}\mathrm{Cu}_{32.6}$ alloy was examined at 1095°C, the $\mathrm{Mn}_{62.6}\mathrm{Sn}_{37.4}$ at 930°C, and an empty quartz container at 975°C, all for 19 hours each, in scans covering $3^\circ < 2\theta < 106^\circ$ in 0.2° steps. The data were analysed using our own programmes taking into account background subtraction, container scattering, absorption, multiple and inelastic scattering. The corrected intensity distributions $I(Q)$ are shown in Figure 1. It was found that these exhibited considerable negative slope. After careful investigation of various experimental effects it was found possible to attribute this slope to paramagnetic scattering from the manganese ions.

The neutron scattering cross-section for paramagnetic scattering is given by

$$\sigma_{pm}(Q) = \frac{8\pi}{3} S(S+1) \left(\frac{e^2\gamma}{mc^2}\right)^2 f_M^2(Q) \tag{5}$$

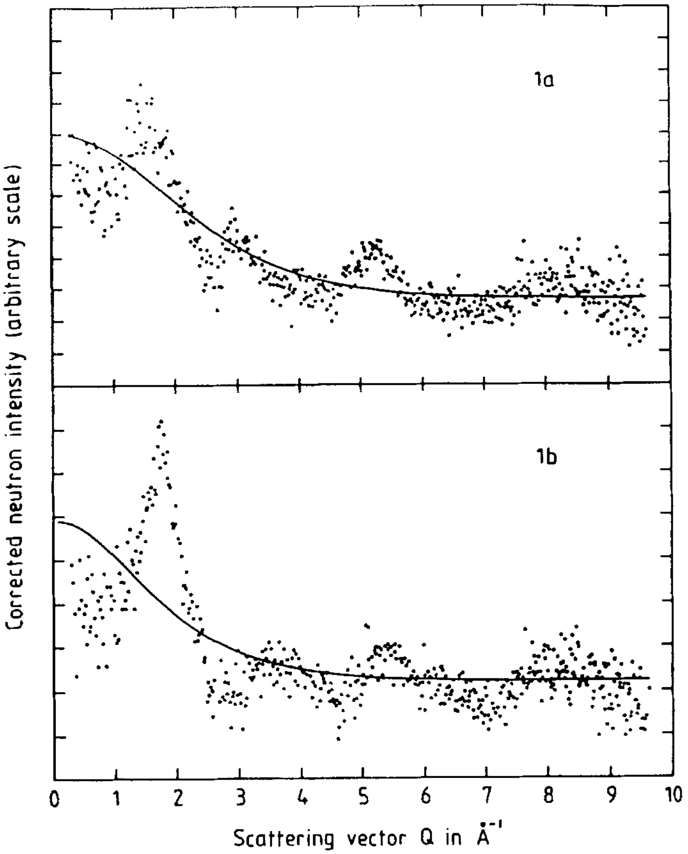

Figure 1 The scattered intensity distributions $I(Q)$ are shown for (1a) $Mn_{67.4}Cu_{32.6}$ and (1b) $Mn_{62.6}Sn_{37.4}$ molten alloys. The considerable slope in these distributions is attributed to paramagnetic scattering from the manganese ions. A normalised form factor for magnetic scattering, see Table 1, is superimposed on the data points.

Table 1 Magnetic moment and magnetic form factor data for manganese ions after Ref. 10.

Ionic state	S value	Magnetic moment in μ_B	Parameters for $f_M(Q)$				
			A	a	B	b	C
Mn^0	5/2	5.9	0.421	0.238	0.579	0.048	−0.007
Mn^+	3	6.9	0.404	0.159	0.596	0.044	−0.010
Mn^{2+}	5/2	5.9	0.371	0.122	0.629	0.040	−0.014
Mn^{3+}	2	4.9	0.384	0.096	0.616	0.036	−0.017

in the usual notation,[9] where $f_M(Q)$ is a form factor for the unpaired electrons. $\sigma_{pm}(Q)$ may be as large as the cross-section for nuclear scattering σ_N, for atoms with a large value of spin S, $f_M(Q)$ may be written

$$f_M(Q) = A \exp(-aQ^2) + B \exp(-bQ^2) + C \tag{6}$$

where the constants A, a, B, b, C have the values given in Table 1.[10] Thus a modified definition of the structure factor $S(Q)$ can be given in this case

$$I(Q) = \langle b^2 \rangle S(Q) + \sigma'_{pm}(Q) \tag{7}$$

where $\sigma'_{p,}(Q) = \sigma_{pm}(Q)/4\pi$ since Eq. (1) has been given, as usual, in terms of $\langle b^2 \rangle$ rather than $\sigma_N = 4\pi\langle b^2 \rangle$. Hence, combining Eqs (4) and (7) gives

$$S_{cc}(Q) = \frac{I(Q) - \sigma'_{pm}(Q)}{\Delta b^2} \tag{8}$$

Four different determinations of $S_{cc}(Q)$ were made using the data in Table 1, to calculate $f_M(Q)$ and hence subtract $\sigma'_{pm}(Q)$ away from $I(Q)$. This was done on a trial and error basis, having regard for the value $\sigma'_{pm}(0)$ and for the fact that the resulting $S_{cc}(Q)$ should oscillate about its limiting value at larger Q values. The best choice for the correction of the magnetic scattering was found using $f_M(Q)$ for the Mn^{2+} ion for the $Mn_{67.4}Cu_{32.6}$ specimen and $f_M(Q)$ for Mn° for the $Mn_{62.5}Sn_{37.5}$ specimen, both of which correspond to magnetic moment values of $5.9\mu_B$. The resulting curves for $\sigma'_{pm}(Q)$ are superimposed on the data points in Figure 1.

There are, in fact, relatively few measurements of the magnetic properties of molten transition metal alloys with which to compare these results. However, Gardner and Flynn[11] have determined a value of 4.4 unpaired electrons per manganese atom in liquid copper, ($\mu = 5.31\mu_B$) in reasonable agreement with the value obtained here, while Ohno[12] has shown that manganese atoms in liquid tin are magnetic and has estimated a moment value $\mu = 4.5\mu_B$, lower than the present one. This estimate was made on the basis of Curie–Weiss behaviour over a limited temperature range. Both of these independent measurements imply that significant magnetic neutron scattering will be observed in experiments on $Mn_{67.4}Cu_{32.6}$ and $Mn_{62.5}Sn_{37.5}$ liquid alloys.

The curves for $S_{cc}(Q)/x(1 - x)$ which result from the subtraction of the paramagnetic scattering are shown in Figure 2. Both curves show the characteristics expected when true short range order exists, namely

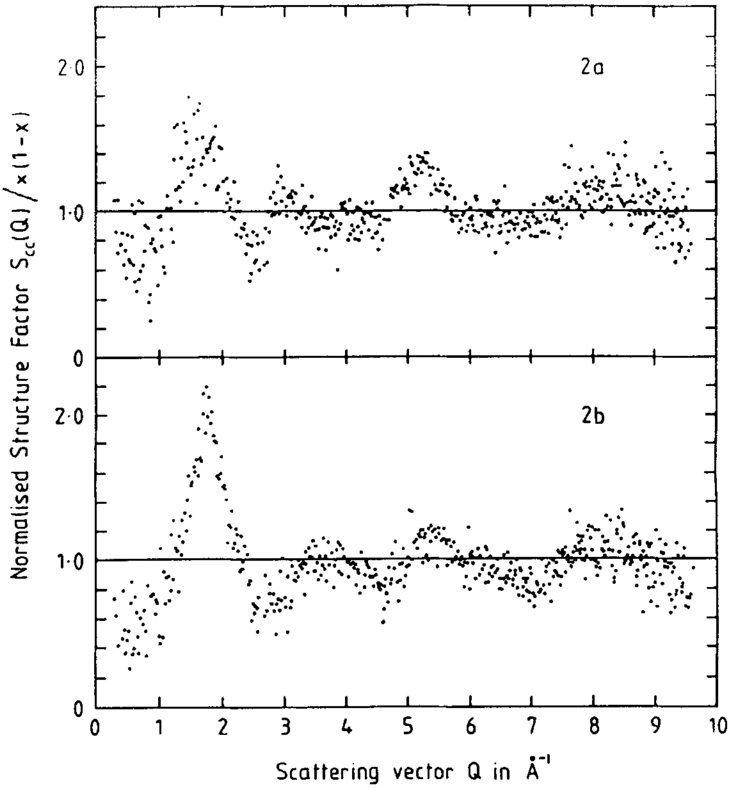

Figure 2 The normalised partial structure factors $S_{cc}(Q)/x(1-x)$ are shown for (2a) $Mn_{67.4}Cu_{32.6}$ and (2b) $Mn_{62.6}Sn_{37.4}$ molten alloys.

a strong peak at small Q values 1.6–1.8 Å^{-1}, the "pre-peak" which provides evidence of *like neighbour* correlations beyond the first neighbour distance, $r_{LN} \sim \frac{5}{4} \cdot 2\pi/Q_{pp} \sim$ 4.4–4.8 Å. The half width of these first peaks, $\Delta Q \sim 0.8$ Å^{-1} indicates a characteristic range for chemical correlations $r_c \sim 2\pi/\Delta Q$ of around 8 Å similar to values obtained by us previously for other molten systems.[3]

3 CHEMICAL SHORT RANGE ORDER IN MOLTEN $Mn_{67.4}Cu_{32.6}$ AND $Mn_{62.6}Sn_{37.4}$ ALLOYS

The radial concentration functions RCFs derived from the Fourier Transform of the curves shown in Figure 2 are given in Figures 3 and 4.

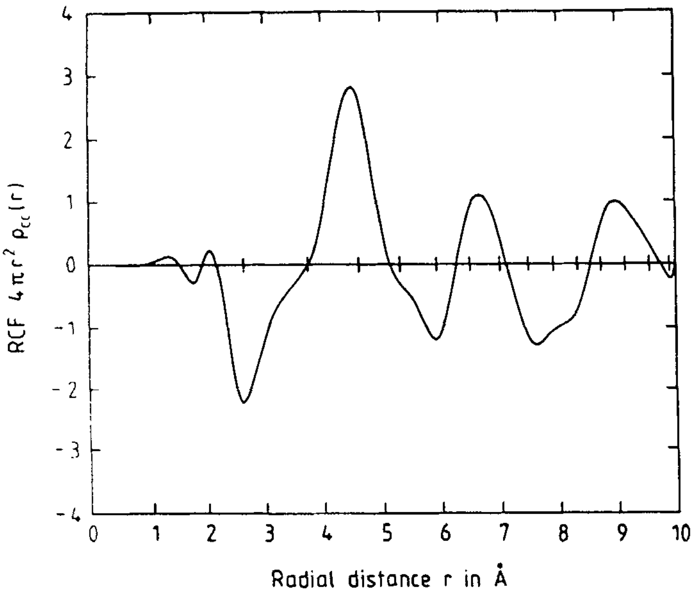

Figure 3 The radial concentration function (RCF) for the $Mn_{67.4}Cu_{32.6}$ alloy obtained from the Fourier transform of the curve in 2a. The short vertical lines on the abscissa give the radial positions of shells of atoms in a hypothetical f.c.c. phase discussed in the text.

The positive and negative peaks in the RCF must clearly correspond to actual interatomic distances in the material and this can be used as a test of the validity of such curves for crystalline specimens.[13] At present, we have been unable to determine the RDF's of the two alloys, say, by a diffraction method with another radiation to make the same kind of identification for the liquid state. However, these RCF's can be discussed in terms of expected first neighbour distances and the atomic correlations in the stable crystalline phases of the two alloys.

The first negative peak in the RCF for $Mn_{67.4}Cu_{32.6}$ at a distance of 2.59 Å is only 2% smaller than the average Goldschmidt diameter of the constituents, 2.64 Å, see Table 2. Assuming a coordination number close to 12, say, $n_1 \sim 11.5$ gives an estimate $\alpha_1 \approx -0.13$ for the CSRO parameter of the first neighbour shell,—which is much lower than the theoretical maximum value,[7] $\alpha_{max} = -x/1 - x = -0.48$. The second, positive, peak in the RCF corresponds to like atom correlations at ~4.5 Å. The Mn-Cu phase diagram[14] shows that below the liquidus temperature the γ-MnCu (f.c.c.) phase is continuous across the diagram for all alloy concentrations. We can postulate a liquid structure based on disordered f.c.c.-like groupings by using the first peak position from

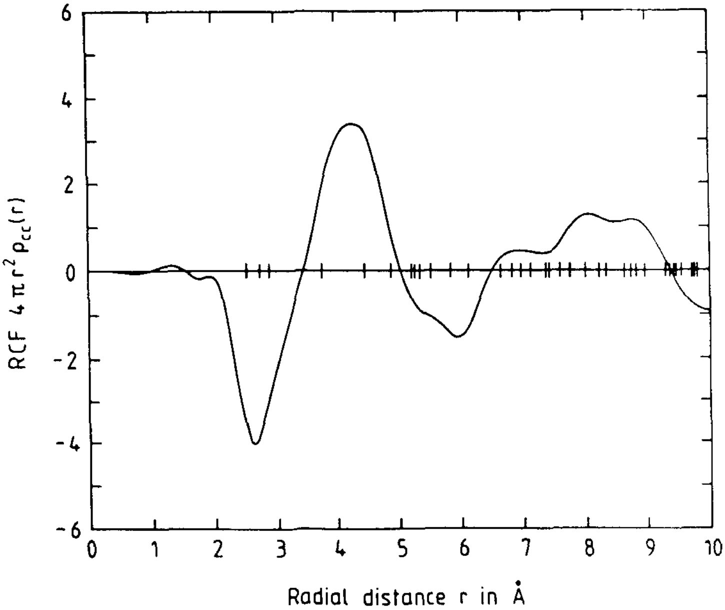

Figure 4 The radial concentration function RCF for the $Mn_{62.6}Sn_{37.4}$ molten alloy obtained from the Fourier transform of the curve in 2b is given. The short vertical lines on the abscissa give radial positions of shells of atoms in the $Mn_{2.05}Sn$ intermetallic compound.

Figure 3, $r_1 = 2.59$ Å, as the first neighbour distance in an f.c.c. cell and calculating all the subsequent distances. An arbitrary stretching factor (2 %) can be included to account for the larger free volume in the liquid phase. The first 14 of such distances are shown in Figure 3 by the short vertical lines on the abscissa. Their overall correspondence with the features of the RCF is surprisingly good. There are, for example, even small features in the RCF as it crosses the abscissa near to the second and fourth interatomic distances. This does not necessarily imply any kind of para-crystalline configuration in the liquid state. The main building blocks of the f.c.c. lattice—tetrahedra and octahedra, are those which are known to predominate (in distorted form as two of the "Bernal Polyhedra") in spatially disordered structures having realistic, soft, potentials, where they occupy up to 90 % of the total volume.[15]

The phase diagram for Mn-Sn shows that several intermetallic compounds form on solidification,[16] of which Mn_2Sn has a range of stability and at $Mn_{2.05}Sn$ has composition close to that of the molten alloy examined here. $Mn_{2.05}Sn$ is based on the $B8_2$ structure, $P6_3/mmc$, No. 194 which has cell dimensions $a = 4.401$ Å and $c = 5.468$ Å,[17] and

Table 2 First neighbour distances and chemical short range order parameter for molten $Mn_{67.4}Cu_{32.6}$ and $Mn_{62.6}Sn_{37.4}$ alloys.

	First neighbour distance in Å		CSRO parameter α_1	
	Observed from RCF	r_1^G	Estimated from RCF	α_{max}
$Mn_{67.4}Cu_{32.6}$	2.59	2.64	−0.13	−0.048
$Mn_{62.6}Sn_{37.4}$	2.65	2.89	−0.25	−0.060

is composed of layers, having triangular and hexagonal configurations of neighbours. A model of this structure was built to investigate the first neighbour shell configurations. The manganese atoms occupy two different sites in the structure having 11 and 14 nearest neighbours at distances of 2.54 Å, 2.73 Å and 2.88 Å of which 5 and 6 respectively are tin atoms. The tin atoms have 11 nearest neighbours of the same distances given above, of which all are manganese. The α_1 values for these sites are -0.377; -0.299 and -0.500 respectively, so that on average $\langle n_1 \rangle = 12$ and $\langle \alpha_1 \rangle = -0.392$.

The RCF for the molten state, Figure 4, has a negative first peak at see Table 2, which covers the three first neighbour distances of the crystalline phase given above. Assuming that the coordination number for the liquid state is also $n_1 \approx 11.5$ gives an estimate $\alpha_1 \approx -0.24$ from Figure 4, which is considerably less than the value for the solid phase and the theoretical maximum value. The $Mn_{2.05}Sn$ crystalline structure also has strong like-atom correlations at 3.73 Å and 4.40 Å and these to are reflected in the positive second peak in the RCF of Figure 4. Interatomic distances in the $Mn_{2.05}Sn$ structure, again stretched by an arbitrary 2% for better comparison with the liquid state, are shown along the abscissa of Figure 4. A close correlation between these longer distances in this phase and the form of the RCF is not expected, although it can be seen that the RCF crosses the abscissa at gaps in the distribution of radial distances except at ~9.3 Å where the correlation has broken down.

Thus leaving aside these longer range correlations, the main conclusion that can be drawn from the description given above, is that in the absence of RDF's for the two molten alloys, the two first peaks of the RCF's are at least consistent with the long range order which develops in the crystalline alloys on solidification.

4 DISCUSSION

More generally, measurements of the enthalpy of mixing of liquid metal alloys can provide information on atomic correlations, through a determination of the sign and magnitude of ΔH. In this case both the experimental conditions and the factors which influence the container material[18] are different from those of neutron work. This makes it worthwhile to compare results on similar samples. The enthalpy of mixing for molten MnSn alloys was measured by Sato and Kleppa[19] and the negative values obtained (e.g. $\Delta H \approx -1.0$ K cal/mol at $Mn_{62.6}Sn_{37.4}$) are in accordance with the negative value of CSRO parameter α_1 obtained here. The situation for molten $Mn_{67.4}Sn_{32.6}$ is less satisfactory, Sato and Kleppa[19] find that ΔH is smaller for Mn-Cu alloys than for Mn-Sn, in keeping with the smaller α_1 value obtained here, but have determined a positive value, $\Delta H \approx 0.30$ kcal/mol for $Mn_{67.4}Cu_{32.6}$. They find that the sign of ΔH changes with composition towards the equiatomic concentrations and this is supported by suggestions that CRSO is solid Mn-Cu alloys also changes in character with composition.[20] In fact examining the sequence of peaks in the RCF of $Mn_{67.4}Cu_{32.6}$, Figure 3, in relation to the proposed interatomic distances suggests α values α_1 $-$ *ve*; $\alpha_2 \sim 0$; α_3 + *ve*; $\alpha_4 \sim 0$ for the first four shells of atoms round an arbitrary origin. This sequence does not correspond to any ordered arrangement which develops in the crystalline alloys on cooling and may be the signature of two competing types of CSRO present.

It is also possible that the Mn-Cu system is less well-characterised than Mn-Sn and Kleppa[21] has, for example, drawn attention to disagreements in the sign of the partial enthalpy of mixing of manganese in copper between experiment and prediction. There appears to be no obvious reason for the agreement between ΔH and α_1 values for $Mn_{62.6}Sn_{37.4}$ and the corresponding disagreement for $Mn_{67.4}Cu_{32.6}$, although a rather unlikely possibility is that magnetic neutron scattering from magnetic atoms which were correlated over short distances might be contributing to the intensity profiles in Figure 1. This could, in principle, be investigated in future experiments using polarised neutron beams.

Acknowledgement

The neutron experiments were made with the support of the Neutron Beam Research Committee of the Science and Engineering Research Council. One of the authors (J-C Li) acknowledges receipt of a Robert Styring Scholarship of the University of Sheffield.

References

1. Ji-chen Li and N. Cowlam, *J. Phys. Chem. Liq.* **17**, 29, 1987.
2. M. Sakata, N. Cowlam and H. A. Davies, Proc. 4th Int. Conf. Rap. Quen. Met. (Sendai: Jap Inst. Met.) **1**, 327, 1982.
3. He Fenglai, N. Cowlam, G. E. Carr and J-B. Suck, *J. Phys. Chem. Liq.*, **16**, 99, 1986.
4. H. A. Davies, *Phys. Chem. Glasses*, **17**, 159, 1976.
5. A. B. Bhatia and D. E. Thornton, *Phys. Rev.*, **B2**, 3004, 1970.
6. J. M. Cowley, *Phys. Rev.*, **77**, 667, 1950.
7. P. Chieux and H. Ruppersberg, *J. Physique*, **C8**, 145, 1980.
8. L. Koesler and W. B. Yelon, *Neut Diff Newsletter*, Int. Union Cryst., 1982.
9. G. E. Bacon, *Neutron Diffraction* (Oxford: Clarendon), 1975.
10. E. J. Lisher and J. B. Forsyth, *Acta. Cryst.*, **A27**, 545, 1971.
11. J. A. Gardner and C. P. Flynn, *Phil. Mag.*, **15**, 1233, 1967.
12. S. Ohno, *J. Non. Cryst. Sol.*, **61 + 62**, 1341, 1984.
13. B. E. Warren, *X-ray diffraction* (Addison-Wesley: Reading, Mass.), 1969.
14. W. G. Moffatt, *The Handbook of Binary Phase Diagrams* (Genium: Schenectady, NY), 1981.
15. J. L. Finney and J. Wallace, *J. Non. Cryst. Sol.*, **43**, 165, 1981.
16. E. A. Brandes and R. F. Flint, *Manganese Phase Diagrams* (Manganese Centre: Paris), 1980.
17. W. B. Pearson, *Handbook of Lattice Spacings and Structures of Metals and Alloys* (Pergamon Press: Oxford), **2**, 1967.
18. O. J. Kleppa and S. Watanabe, *Met. Trans.*, **13B**, 391, 1982.
19. S. Sata and O. J. Kleppa, *Met. Trans.*, **10B**, 63, 1979.
20. N. Cowlam and A. M. Shamah, *J. Phys. F: Met. Phys.*, **11**, 27, 1981.
21. O. J. Kleppa, *J. Non. Cryst. Sol.*, **61 + 62**, 101, 1984.